Modeling and Inference of Sparse Neural Dynamic Functional Connectivity Networks Underlying Functional Ultrasound Data

Wijnands, Ruben; Dauwels, Justin; Serra, Ines; Kruizinga, Pieter; Badura, Aleksandra; Hunyadi, Borbala

Citation (APA)
Wijnands, R., Dauwels, J., Serra, I., Kruizinga, P., Badura, A., & Hunyadi, B. (2023). Modeling and Inference of Sparse Neural Dynamic Functional Connectivity Networks Underlying Functional Ultrasound Data. In *ICASSPW 2023 - 2023 IEEE International Conference on Acoustics, Speech and Signal Processing Workshops, Proceedings* (ICASSPW 2023 - 2023 IEEE International Conference on Acoustics, Speech and Signal Processing Workshops, Proceedings). IEEE. https://doi.org/10.1109/ICASSPW59220.2023.10193029

Important note
To cite this publication, please use the final published version (if applicable).
Please check the document version above.

MODELING AND INFERENCE OF SPARSE NEURAL DYNAMIC FUNCTIONAL CONNECTIVITY NETWORKS UNDERLYING FUNCTIONAL ULTRASOUND DATA

Ruben Wijnands[1], *Justin Dauwels*[1], *Ines Serra*[2],
Pieter Kruizinga[2], *Aleksandra Badura*[2] and *Borbála Hunyadi*[1]

[1]Department of Microelectronics, Delft University of Technology, Delft, The Netherlands
[2]Department of Neuroscience, Erasmus Medical Center, Rotterdam, The Netherlands

ABSTRACT

Functional ultrasound (fUS) is a novel neuroimaging technique that measures brain hemodynamics through a time series of Doppler images. The measured spatiotemporal hemodynamic changes reflect changes in neural activity through the neurovascular coupling (NVC). Often, such image time series is used to analyze dynamic functional connectivity (dFC) by directly computing a connectivity metric between the measured hemodynamic signals, ignoring the functional connectomics of underlying neural populations. This work proposes a novel fUS signal model, consisting of a hidden Markov model (HMM) cascaded with a convolutive model, that captures how fUS signals arise from a generative perspective while incorporating high-level biological functioning of neural populations. Consequently, the developed model enables inference of functional connectivity networks, being co-activation patterns (CAPs) of neural populations. Our results show that our methods can identify biologically plausible networks of functional connectivity. Furthermore, this method captures a difference in brain dynamics between wild-type and *Shank2*$^{-/-}$ mouse mutants.

Index Terms— Dynamic functional connectivity, functional ultrasound, deconvolution, hidden Markov models, co-activation patterns

1. INTRODUCTION

Functional neuroimaging focuses on revealing physiological changes in the brain in order to obtain a better understanding of its function. With the introduction of functional imaging techniques, the functional connectome has been increasingly researched. Functional connectivity can be defined as the statistical relationship between signals measured at different brain regions of interest (ROIs) [1]. Multiple regions that are functionally connected comprise a so-called functional network. Until recently, the stationarity of these networks was

assumed. However, the signature of these networks is changing dynamically in time [1, 2]. This discovery led to the development of dynamic functional connectivity (dFC), in which changes in functional connectivity of networks are measured. Measures of (dynamic) functional connectivity have proven useful in characterizing abnormalities in brain connectivity. For example, altered connectivity patterns in disorders such as autism spectrum disorder (ASD) have been identified in humans and mice [3, 4]. Identifying disorder-specific functional connectivity alterations can help understand the origin of such disorders to improve diagnosis and eventually lead to better treatment options.

Functional ultrasound (fUS) is a relatively new neuroimaging technique that measures hemodynamic changes proportional to the moving cerebral blood volume (CBV) [5, 6]. The measured changes are related to the underlying activity of neural populations through the neurovascular coupling (NVC) mechanism. When a brain region activates, an increased blood flow provides the region with, amongst others, oxygen and glucose to maintain the homeostasis of the cerebral micro-environment [7]. As fUS records activity of multiple brain regions simultaneously, functional connectivity patterns can be identified. However, since fUS is a relatively new imaging technique, there are only a handful of contributions to analyzing (dynamic) functional connectivity. In the work of [8, 9], static functional connectivity patterns are revealed. In addition, dFC has been analyzed using k-means clustering of phase coherence matrices in [10, 11].

It should be noted that all previously mentioned works compute a metric of functional connectivity using the measured fUS signals directly. However, from a biological perspective, functional connectivity occurs at the neural level [12]. Therefore, in this paper, functional connectivity is measured as the co-activation of underlying neural populations, named ROIs, instead of the statistical relationship between time courses of ROIs. We expect that through reconstructing and identifying the underlying neural co-activation patterns (CAPs), a more accurate and biologically plausible representation of functional connectivity networks and their fast dynamics can be obtained.

In the context of functional magnetic resonance imaging (fMRI), it is indeed found that functional networks, previously inferred from conventional correlation analysis, are driven by activity at only a few critical time points using CAP detection [2, 13]. In the work of [14], CAPs are detected by clustering innovation signals, being derivatives of total activation (TA) deconvolved time courses. Then, by using a back-projection step, block-type neural signals are obtained. Concerning brain network dynamics, the authors of [15] deploy the hidden Markov model (HMM) on fMRI time courses directly, revealing that brain states are temporally organized. Also, nonrandom sequencing of brain networks has been revealed at the neural basis of fMRI using simultaneous EEG-fMRI measurements in [16].

In this work, we develop a novel two-stage generative fUS signal model consisting of an HMM cascaded with a convolutive model. As an additional novelty, we propose nonnegative paradigm free mapping (PFM) to reconstruct time courses of neural activity, inspired by the signatures of neural population time courses in [17]. As CAPs enable a framewise analysis approach, we leverage the relatively high temporal resolution of fUS imaging and research the fast brain dynamics in mice.

2. FUNCTIONAL ULTRASOUND DATA MODELING

In this section, we construct an fUS signal model comprising two cascaded stages. The first stage consists of a generative model to provide insight into the recurring CAPs of underlying neural activity and their transitional preferences. The second stage of the signal model consists of a convolutive signal model, relating the underlying neural activity to the measured fUS signals.

2.1. Generative modeling of neural population activity

The neural activity amplitude, underlying the fUS data, of an ROI $m \in \{1, ..., M\}$ over discrete time $n \in \{1, ..., N\}$, is denoted by vector $\mathbf{y}_m \in \mathbb{R}^N$. Then, having neural activity patterns of multiple ROIs, matrix $\mathbf{Y} = [\mathbf{y}_1, \mathbf{y}_2, ..., \mathbf{y}_M]$ is constructed. Now, the co-activations of ROIs can be recognized in the rows of matrix $\mathbf{Y}$, denoted by $\mathbf{y}_n \in \mathbb{R}^M$, that are assumed to be constant within a time-bin equal to the sampling period. The co-activation vector $\mathbf{y}_n$ can be considered a multivariate random variable, where matrix $\mathbf{Y}$ is a realization of a stochastic process Y. The distribution from which $\mathbf{y}_n$ is generated can change over time, as various co-activation patterns may be present between the ROIs, ultimately leading to a non-stationary stochastic process Y.

As a next step, a probabilistic structure is imposed between the different co-activation patterns via the well-known HMM structure. The realization $\mathbf{z} = [z_1, z_2, ..., z_N]$ of the latent stochastic process Z, indicates the presence of a particular composition of active ROIs. Each z_n comes from a discrete state-space $\mathcal{S} = \{1, ..., K\}$, which labels the co-activation patterns $\mathbf{y}_n$, and only one state $z_n \in \mathcal{S}$ can be active at a time. The state transitions are governed by a state transition probability matrix $\mathbf{A}$, containing elements

$$a_{ij} = P(z_{n+1} = j | z_n = i). \tag{1}$$

Thus, this process can be recognized as a first-order discrete-time Markov chain, and the HMM framework establishes itself by relating the random co-activity vector $\mathbf{y}_n$ to the hidden process Z. For the Gaussian HMM, in which each state generates emissions from a state-specific multivariate Gaussian distribution, the vector $\mathbf{y}_n$ is conditionally dependent only on z_n:

$$p(\mathbf{y}_n | z_n = i) \sim \mathcal{N}(\boldsymbol{\mu}_{z_n}, \boldsymbol{\Sigma}_{z_n}), \tag{2}$$

where $\boldsymbol{\mu}_{z_n} \in \mathbb{R}^M$ and $\boldsymbol{\Sigma}_{z_n} \in \mathbb{R}^{M \times M}$. Thus, the functional connectivity pattern is captured by the mean $\boldsymbol{\mu}_{z_n}$ of the multivariate Gaussian distribution. This finally results in a mixture of multivariate Gaussian distributions for all possible states in $\mathcal{S}$. The high-level biological functioning of neural populations is incorporated into the model since it allows a specific CAP to have various amplitudes, which is logical as an ROI always contains multiple neurons. Also, no activity is present when an ROI has zero amplitude.

2.2. Convolutive fUS signal model

The observed fUS signals $\mathbf{F} \in \mathbb{R}^{N-L+1 \times M}$ are modeled as the convolution of the CAPs in $\mathbf{Y}$ and the causal Toeplitz LTI filter matrix $\mathbf{H} \in \mathbb{R}^{N-L+1 \times N}$, modeling the NVC:

$$\mathbf{F} = \mathbf{H}\mathbf{Y} + \mathbf{N}. \tag{3}$$

The observed fUS signals also contain noise, represented by matrix $\mathbf{N} = [\boldsymbol{\epsilon}_1, \boldsymbol{\epsilon}_2, ..., \boldsymbol{\epsilon}_M]$ with columns following an i.i.d. Gaussian white noise process $\epsilon_{n,m} \sim \mathcal{N}(0, \sigma^2)$. The rows of $\mathbf{H}$ contain the hemodynamic response function (HRF) $\mathbf{h} \in \mathbb{R}^L$, representing the transfer function linking neural activity with the fUS signals, and having entries

$$h_l = p_3(\Gamma(p_1))^{-1}(t_l)^{p_1-1}p_2^{p_1}e^{-p_2 t_l}, \tag{4}$$

where $l \in \{0, ..., L-1\}$, and $t_l = lT_s$ with T_s being the sampling period. Furthermore, parameters p_1 and p_2 determine the shape of the HRF, and p_3 scales the HRF to unit amplitude without loss of generality.

3. METHODS

3.1. Deconvolution

A deconvolution procedure is used to estimate the underlying neural activity per ROI m. As demonstrated in (5), regularization is performed via the least absolute shrinkage and selection operator to solve the originally ill-posed problem of re-

constructing $\mathbf{y}_m$. Now, we expand PFM [18] to non-negative PFM by the addition of a non-negativity constraint.

$$\hat{\mathbf{y}}_m = \arg\min_{\mathbf{y}_m} \quad \frac{1}{2N}||\mathbf{f}_m - \mathbf{H}\mathbf{y}_m||_2^2 + \lambda||\mathbf{y}_m||_1 \quad (5)$$
$$\text{s.t.} \quad \mathbf{y}_m \geq 0.$$

3.2. Inference of functional networks

For the HMM inference of functional networks from the reconstructed matrix $\hat{\mathbf{Y}} = [\hat{\mathbf{y}}_1, \hat{\mathbf{y}}_2, ..., \hat{\mathbf{y}}_M]$, we deploy the Baum-Welch algorithm, being an instance of the expectation maximization (EM) algorithm, by using the implementation of [19]. We initialize the EM algorithm by k-means clustering of observations. Furthermore, the initial probabilities π and state transition probability matrix $\mathbf{A}$ are uniformly initialized. For the EM procedure, we use 50 iterations to learn the model parameters, sufficient for convergence of the model log-likelihood in practice. Finally, Viterbi decoding is applied to infer the most probable state sequence $\mathbf{z}$.

4. RESULTS

In this section, simulation and experimental data results are presented. Through a brief simulation, we analyze the ability to recover true functional networks and the influence of noise on the state transition probability matrix $\mathbf{A}$. Subsequently, we test the developed model and methods on experimental data, analyzing dFC in normal and mutated mice. [1]

4.1. Simulation

Synthetic data is generated by creating a bivariate binary state pattern consisting of $K = 3$ states, depicted in Fig. 1a. This synthetic state pattern follows the state transition probability matrix of Fig. 1c. Subsequently, bivariate synthetic fUS data is generated according to (3), with intensity $\sigma = 0.5$.
After deconvolution and state-space inference on synthetic data, the correct CAPs were inferred. The inferred transition probability matrix in Fig. 1d shows reduced transition probabilities concerning the second and third state and increased transition preference to the first state due to sparse regularization on noisy synthetic data. However, the main trends, being state self-transitions and transitional preference from state two to state three, are still visible.

4.2. Experimental data

The experimental data set on which we test the developed model and methods consists of four wild-type mice and four *Shank2*^{-/-} mutant mice. This mutation results in autistic-like behavior and is often used in ASD research. At the Center for

---

[1]Code and additional information on the analysis available at: https://github.com/rubenwijnands999/dFC-fUS
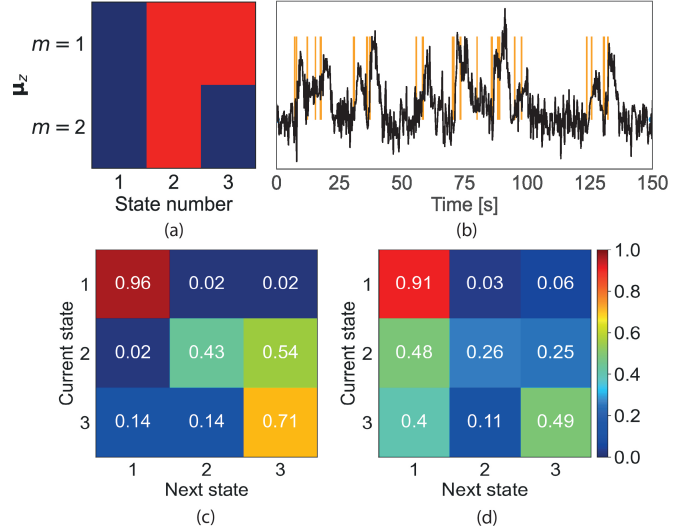

Fig. 1. Synthetic data generation and inference. (a) Synthetic states $K = 3$ with active (red) and not active (blue) patterns, involving $M = 2$ ROIs. (b) Example binary activation pattern $\mathbf{y}_m$ (orange) and synthetic noisy fUS time course $\mathbf{f}_m$ with $\sigma = 0.5$ (black). True (c) and inferred (d) state transition probability matrix.

Ultrasound and Brain imaging at Erasmus MC (CUBE), 12-minute recordings consisting of 2D power Doppler images (PDIs) have been acquired at a sampling rate of 4 Hz. Specifically, the brain section containing the thalamus and motor cortex has been imaged. During fUS acquisition, the mice were head-fixed yet freely moving on a running wheel. We investigate whether our developed methods can reveal a difference in brain dynamics between the two groups of mice.

The fUS data is pre-processed as follows. First, the pixels belonging to $M = 3$ ROIs are identified by performing a spatial independent component analysis (sICA), with model order $C = 25$, and thresholding the pixels of the independent spatial components within a warped Allen Mouse Brain Atlas. Subsequently, the mean fUS time course is computed for each ROI, and the baseline of the result is centered around the zero axis.

Then, for each group of mice, an HMM inference procedure with $K = 4$ is applied on the concatenated time courses obtained from non-negative PFM deconvolution. The inferred functional networks, shown in Fig. 2a, appeared to be similar for each group of mice and are consistent across subsampled data sets and different initializations of the EM algorithm. Furthermore, this decomposition of neural activity is biologically plausible [17, 20]. For comparison, we also applied non-negative TA deconvolution, as demonstrated in Fig. 2b. However, state-space inference did not result in a decomposition of the all-active brain state (state number two in Fig. 2a). Rather, it resolved multiple all-active brain states with different activity levels (not shown).
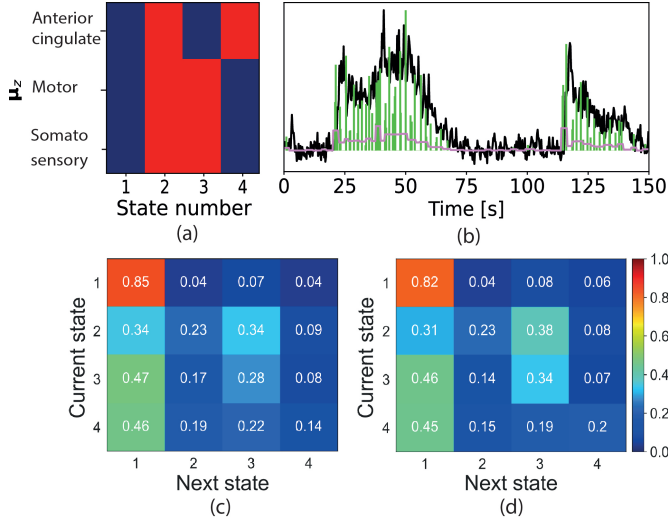
Fig. 2. Inference on experimental fUS data. (a) Inferred functional connectivity networks (thresholded) of both wild-type and *Shank2⁻/⁻* mutant mice, with active (red) and not active (blue) brain regions. (b) mean fUS time course of the motor region (black) with deconvolved time course using non-negative PFM (green) and TA (purple). State transition probability matrices of (c) wild-type and (d) *Shank2⁻/⁻* mutant mice.

As shown in Fig. 2c-d, the transitional dynamics are also similar across the groups, except for altered transition probabilities between states 2 and 3, of which the effect is further investigated. To analyze the genuineness of the observed effect, we performed 500 Monte Carlo experiments. In each Monte Carlo experiment, two random groups of fUS recordings are made, and an HMM inference procedure is applied for each random group. Then, the inferred state transition probability matrices that only contain the second and third state are re-scaled such that the rows sum to unit probability. Finally, the mean squared error (MSE) between both sub-matrices is computed, resulting in 96.8% of the Monte Carlo experiments having a lower measured effect than the actual effect.

5. DISCUSSION

This paper presented a novel approach to inferring dynamic functional networks from fUS data, through modeling fUS data from a generative perspective, using an HMM cascaded with a convolutive model. In fMRI deconvolution procedures, typically activation and de-activation patterns are k-means clustered, being deviations from a baseline neural activity [14]. Motivated by [17], this work proposes a framework more closely related to the high-level functioning of neural populations. This novelty is incorporated in the non-negativity constraint of the deconvolution procedure, being an expansion of the well-known PFM [18]. Furthermore, instead of k-means clustering, we infer a finite number

of CAPs using an HMM structure, assuming a probabilistic transitional structure between functional networks. This spatiotemporal clustering approach using Gaussian distributions is advantageous in practice as it allows a specific CAP to have various amplitudes, yet it also learns clusters that show a clear separation between active and non-active brain regions.

It appears that our model and methods can explain fUS data, as biologically plausible functional networks are inferred, and a significant difference in brain dynamics between wild-type and *Shank2⁻/⁻* mutant mice is shown. However, using non-negative TA deconvolution, we did not obtain similar functional networks. This could be explained by the fact that TA regularizes the solution with smoothness, and thereby does not emphasize short instances of neural activity. In Fig. 2b, it is also visible that TA deconvolved time courses generally follow the main trends of the fUS time course.

For future work, it is recognized that a joint multivariate deconvolution procedure and CAP inference approach could improve the developed methodology by obtaining a global solution to the problem of inferring functional networks from data. Also, information captured by Σ_{z_n} or its inverse could be further exploited, being a measure of connectivity upon a certain CAP.

Lastly, our method has a few tunable parameters. For creating the HRF, we used $L = 33$, $p_1 = 4.00$, $p_2 = 1.50$, and $p_3 = 2.98$, such that the HRF shape is similar to the HRF presented in [21]. Furthermore, we select λ such that the error $||\mathbf{f}_m - \mathbf{H}\hat{\mathbf{y}}_m||_2^2$ does not exceed a percentage threshold of 1% between a non sparse solution, also recognized as a non-negative least squares (NNLS) solution, and an extremely sparse solution, i.e., $\mathbf{y}_m = \mathbf{0}$. Also, the number of states K was motivated by the empirical observation of biologically plausible networks. We tested different values for K, resulting in no significant differences in the fractional occupancy of states, mean state life time, and mean inter-state time.

6. CONCLUSION

We developed an fUS signal model and leveraged methods that allow for reconstructing dynamic functional connectivity networks from fUS measurements in terms of the co-activation patterns of underlying neural activity. The model consists of an HMM cascaded with a convolutive model, and the methods comprise a deconvolution procedure and state-space inference approach. In a simulation study, we showed that although noisy measurements influence reconstructed neural activity, the derived networks and the main trends in the inferred transition probability matrix are reliable. Our method inferred biologically plausible functional networks in an experimental data set investigating brain activity of wild-type and *Shank2⁻/⁻* mutant mice. Also, we observed a transitional bias towards the functional network comprising the motor and somatosensory cortices in *Shank2⁻/⁻* mutant mice, related to the mutation with 96.8% certainty.

7. REFERENCES

[1] R. M. Hutchison, T. Womelsdorf, E. A. Allen, P. A. Bandettini, V. D. Calhoun, et al., "Dynamic functional connectivity: Promise, issues, and interpretations," *NeuroImage*, vol. 80, pp. 360–378, 10 2013.

[2] X. Liu and J. H. Duyn, "Time-varying functional network information extracted from brief instances of spontaneous brain activity," *Proceedings of the National Academy of Sciences of the United States of America*, vol. 110, no. 11, pp. 4392–4397, 3 2013.

[3] C. J. Stoodley, A. M. D'Mello, J. Ellegood, V. Jakkamsetti, P. Liu, et al., "Altered cerebellar connectivity in autism and cerebellar-mediated rescue of autism-related behaviors in mice," *Nature Neuroscience*, vol. 20, no. 12, pp. 1744–1751, 12 2017.

[4] V. Zerbi, M. Pagani, M. Markicevic, M. Matteoli, D. Pozzi, et al., "Brain mapping across 16 autism mouse models reveals a spectrum of functional connectivity subtypes," *Molecular Psychiatry*, vol. 26, no. 12, pp. 7610–7620, 12 2021.

[5] E. Mace, G. Montaldo, B. F. Osmanski, I. Cohen, M. Fink, et al., "Functional ultrasound imaging of the brain: Theory and basic principles," *IEEE Transactions on Ultrasonics, Ferroelectrics, and Frequency Control*, vol. 60, no. 3, pp. 492–506, 2013.

[6] T. Deffieux, C. Demené, and M. Tanter, "Functional Ultrasound Imaging: A New Imaging Modality for Neuroscience," *Neuroscience*, vol. 474, pp. 110–121, 2021.

[7] C. Iadecola, "The Neurovascular Unit Coming of Age: A Journey through Neurovascular Coupling in Health and Disease," *Neuron*, vol. 96, no. 1, pp. 17–42, 9 2017.

[8] B. F. Osmanski, S. Pezet, A. Ricobaraza, Z. Lenkei, and M. Tanter, "Functional ultrasound imaging of intrinsic connectivity in the living rat brain with high spatiotemporal resolution," *Nature Communications*, vol. 5, 2014.

[9] A. Bergel, T. Deffieux, C. Demené, M. Tanter, and I. Cohen, "Local hippocampal fast gamma rhythms precede brain-wide hyperemic patterns during spontaneous rodent REM sleep," *Nature Communications*, vol. 9, no. 1, 12 2018.

[10] L. Rahal, M. Thibaut, I. Rivalse, J. Claron, Z. Lenkei, et al., "Ultrafast ultrasound imaging pattern analysis reveals distinctive dynamic brain states and potent subnetwork alterations in arthritic animals," *Scientific Reports*, vol. 10, no. 1, 12 2020.

[11] J. Baranger, C. Demené, A. Frerot, F. Faure, C. Delanoë, et al., "Bedside functional monitoring of the dynamic brain connectivity in human neonates," *Nature Communications*, vol. 12, no. 1, 12 2021.

[12] G. J. Thompson, M.D. Merritt, W. Pan, M. E. Magnuson, J. K. Grooms, et al., "Neural correlates of time-varying functional connectivity in the rat," *NeuroImage*, vol. 83, pp. 826–836, 2013.

[13] X. Liu, C. Chang, and J. H. Duyn, "Decomposition of spontaneous brain activity into distinct fmri co-activation patterns," *Frontiers in Systems Neuroscience*, vol. 7, 2013.

[14] F. I. Karahanoglu and D. van de Ville, "Transient brain activity disentangles fMRI resting-state dynamics in terms of spatially and temporally overlapping networks," *Nature Communications*, vol. 6, 7 2015.

[15] Diego Vidaurre, Stephen M. Smith, and Mark W. Woolrich, "Brain network dynamics are hierarchically organized in time," *Proceedings of the National Academy of Sciences*, vol. 114, no. 48, pp. 12827–12832, 11 2017.

[16] B. Hunyadi, M. W. Woolrich, A. J. Quinn, D. Vidaurre, and M. De Vos, "A dynamic system of brain networks revealed by fast transient EEG fluctuations and their fMRI correlates," *NeuroImage*, vol. 185, pp. 72–82, 1 2019.

[17] C. Stringer, M. Pachitariu, N. A. Steinmetz, C. B. Reddy, M. Carandini, et al., "Spontaneous behaviors drive multidimensional, brainwide activity," *Science*, vol. 364, no. 6437, 2019.

[18] C. C. Gaudes, N. Petridou, I. L. Dryden, L. Bai, S. T. Francis, et al., "Detection and characterization of single-trial fmri bold responses: Paradigm free mapping," *Human Brain Mapping*, vol. 32, no. 9, pp. 1400–1418, 2011.

[19] S. Linderman, B. Antin, D. Zoltowski, and J. Glaser, "SSM: Bayesian Learning and Inference for State Space Models," 2020.

[20] N. A. Steinmetz, P. Zatka-Haas, M. Carandini, and K. D. Harris, "Distributed coding of choice, action and engagement across the mouse brain," *Nature*, vol. 576, no. 7786, pp. 266–273, 12 2019.

[21] A. O. Nunez-Elizalde, M. Krumin, C. B. Reddy, G. Montaldo, A. Urban, et al., "Neural correlates of blood flow measured by ultrasound," *Neuron*, 3 2022.